4ICEGE Thessaloniki-GREECE 2007

4th International Conference on
Earthquake Geotechnical Engineering
June 25-28, 2007
Paper No. 1707

NUMERICAL PREDICTION OF GROUND VIBRATIONS DUE TO PILE DRIVING USING A HYBRID FORMULATION

H.R. Masoumi, S. François, G. Degrande

ABSTRACT

This work aims to develop a numerical model to predict free field vibrations due to vibratory and impact pile driving. For this purpose, a hybrid frequency-time domain formulation is presented. Based on a coupled FE-BE approach, the soil-pile system is decomposed into two subdomains: (a) a finite domain containing the pile and a part of the soil that can behave non-linearly and (b) the unbounded semi-infinite linear soil domain. The unbounded soil region is represented by tractions at the soil-structure interface in terms of stiffness matrices and displacements, which are added to the equation of motion of the finite domain. The stiffness or flexibility matrices of the unbounded soil are computed in the frequency domain by means of a boundary element method. Using a hybrid approach and a Fourier transformation of the flexibility matrix to the time domain, the force-displacement relationship is obtained in the time domain. Newmark's time integration scheme is used to solve the equation of motion of the coupled system. Results of the present method under linear behaviour are compared with those obtained by a frequency domain analysis.

Keywords: dynamic soil-structure interaction, hybrid method, coupled FE-BE method, pile driving

INTRODUCTION

Due to the non-linear constitutive behaviour of the soil surrounding the pile, the dynamic soil-pile interaction problem is non-linear and must be analysed in the time domain.

In recent years, many researchers have dealt with the analysis of dynamic soil-pile interaction problems in the time domain (Mamoon & Banerjee, 1992; Tham, et al., 1996). Some progress has been also made by developing models to assess the driving efficiency of driven piles using a non-linear constitutive law for the soil (Holeyman, 2002). In particular, some works are based on the application of the time domain boundary element method with the fundamental solutions for the dynamic soil-structure interaction problems (Wolf, 1988; Bode, et al., 2002).

Using a substructuring method, the soil-structure system is decomposed into two independent substructures: (a) the inhomogeneous or non-linear structure, and (b) the unbounded linear elastic soil. For each of these substructures, the basic dynamic equilibrium equations are written independently. The properties of the unbounded soil (linear part) on the exterior are represented by a boundary condition in the form of a force-displacement relationship, which is global in space and time. This relationship is expressed in the form of convolution integrals involving the dynamic stiffness coefficients in the time domain with respect to the degrees of freedom of the nodes located on the soil-structure interface. Alternatively, Green's functions in the time domain can be directly used in the computational procedure.

As it is assumed that the unbounded soil on the exterior of the interaction horizon up to infinity behaves linearly, this substructure can be analyzed in the frequency domain. The dynamic impedance of the

Structural Mechanics, K.U.Leuven, Belgium, Email: hamidreza.masoumi@bwk.kuleuven.be

soil is calculated by means of a boundary element formulation that employs the Green's functions of a horizontally stratified soil.

An alternative consists in calculating the unbounded soil's interaction forces in the frequency domain and transforming these into the time domain. These forces are subsequently used to solve the interaction problem in the time domain (Wolf, 1988). This strategy is referred to as a hybrid frequency-time domain approach, while the direct formulation in the time domain is called the direct time domain approach.

Wolf (1988) has proposed several alternatives to formulate the soil-structure interaction forces in the time domain. In order to avoid the difficulties associated with the transformation of the dynamic-stiffness coefficients, a flexibility formulation is used in this work (François & Degrande, 2005).

Finally, the interaction forces in the time domain are added to the nodes of the soil-structure interface and the equation of the motion of the generalized structure is solved by means of Newmark's time integration method.

NUMERICAL MODELING

Problem outline

As the main objective of this work is the time domain analysis of the dynamic soil-pile interaction problem during pile driving, the governing equations are presented for an embedded pile in a homogeneous layered soil medium.

First, the soil-structure system is decomposed into two subdomains: the bounded (generalised) structure Ω_b that contains the pile and an irregular soil region adjacent to the pile which can behave non-linearly, and the unbounded semi-infinite layered soil denoted by Ω_s^{ext}. The interface between the bounded (structure) and unbounded (linear soil) subdomain is denoted by Σ, as shown in figure 1a.

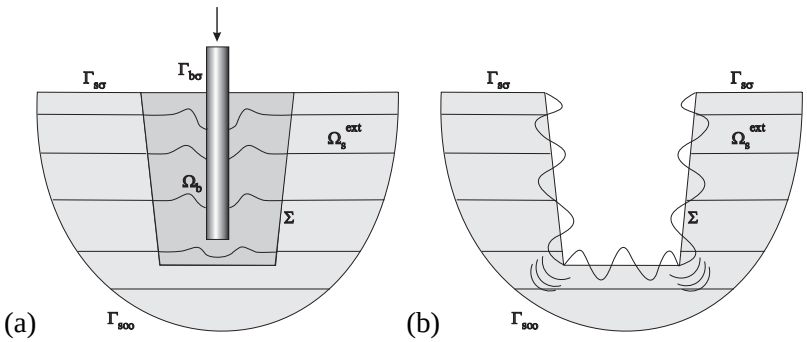

Figure 1: (a) The geometry of the problem, and (b) the radiated wave fields $\mathbf{u}_{\text{sc}}(\mathbf{u}_b)$.

Equilibrium equations in the structure

First, the structure Ω_b is considered. The boundary $\Gamma_b = \Gamma_{b\sigma} \cup \Sigma$ of the bounded domain Ω_b is decomposed into a boundary $\Gamma_{b\sigma}$ where tractions $\bar{\mathbf{t}}_b$ are imposed and the soil-structure interface Σ. The displacement vector $\mathbf{u}_b$ of the structure satisfies the following Navier equation and boundary conditions:

$$\operatorname{div} \boldsymbol{\sigma}_b(\mathbf{u}_b) + \rho_b \mathbf{b} = \rho_b \ddot{\mathbf{u}}_b \qquad \text{in } \Omega_b \tag{1}$$

$$\mathbf{t}_b(\mathbf{u}_b) = \bar{\mathbf{t}}_b \qquad \text{on } \Gamma_{b\sigma} \tag{2}$$

$$\tag{3}$$

where $\rho_b \mathbf{b}$ denotes the body force on the structure and $\mathbf{t}(\mathbf{u}) = \boldsymbol{\sigma}(\mathbf{u}) \cdot \mathbf{n}$ the traction vector on a boundary with a unit outward normal vector $\mathbf{n}$.

Equilibrium equations in the soil

The exterior soil domain Ω_s^{ext} is taken into consideration. The boundary $\Gamma_s^{\text{ext}} = \Gamma_{s\sigma} \cup \Gamma_{s\infty} \cup \Sigma$ of the soil domain Ω_s^{ext} is decomposed into the boundary $\Gamma_{s\sigma}$ where tractions are imposed, the outer boundary $\Gamma_{s\infty}$ where radiation conditions are satisfied and the soil-structure interface Σ. Free boundary conditions or zero tractions are assumed on $\Gamma_{s\sigma}$. The displacement vector $\mathbf{u}_s$ of the soil satisfies the Navier equation and the following boundary conditions:

$$\operatorname{div} \boldsymbol{\sigma}_s(\mathbf{u}_s) = \rho_s \ddot{\mathbf{u}}_s \qquad \text{in } \Omega_s^{\text{ext}} \tag{4}$$

$$\mathbf{t}_s(\mathbf{u}_s) = \mathbf{0} \qquad \text{on } \Gamma_{s\sigma} \tag{5}$$

$$\mathbf{u}_s = \mathbf{u}_b \qquad \text{on } \Sigma \tag{6}$$

$$\mathbf{t}_b(\mathbf{u}_b) + \mathbf{t}_s(\mathbf{u}_s) = \mathbf{0} \qquad \text{on } \Sigma \tag{7}$$

According to the compatibility condition (6), the displacement vector $\mathbf{u}_s$ is equal to the scattered wave field $\mathbf{u}_{\text{sc}}(\mathbf{u}_b)$ radiated in the soil due to the motion $\mathbf{u}_b$, imposed on the interface Σ (figure 1b):

$$\mathbf{u}_s = \mathbf{u}_{\text{sc}}(\mathbf{u}_b) \qquad \text{in } \Omega_s^{\text{ext}} \tag{8}$$

Variational formulation

The equation of the motion of the dynamic soil-structure interaction problem is formulated in a variational form. For any virtual displacement field $\delta\mathbf{v}$ imposed on the structure, the sum of the virtual work of the internal and the inertial forces is equal to the virtual work of the external loads:

$$\int_{\Omega_b} \boldsymbol{\varepsilon}(\delta\mathbf{v}) : \boldsymbol{\sigma}_b(\mathbf{u}_b) d\Omega + \int_{\Omega_b} \delta\mathbf{v} \cdot \rho_b \ddot{\mathbf{u}}_b d\Omega = \int_{\Omega_b} \delta\mathbf{v} \cdot \rho_b \mathbf{b} d\Omega + \int_{\Gamma_{b\sigma}} \delta\mathbf{v} \cdot \bar{\mathbf{t}}_b d\Gamma + \int_{\Sigma} \delta\mathbf{v} \cdot \mathbf{t}_b(\mathbf{u}_b) d\Sigma \tag{9}$$

Accounting for the equilibrium of the tractions on the soil-structure interface Σ, the variational equation (9) becomes (in the absence of the body forces):

$$\int_{\Omega_b} \boldsymbol{\varepsilon}(\delta\mathbf{v}) : \boldsymbol{\sigma}_b(\mathbf{u}_b) d\Omega + \int_{\Omega_b} \delta\mathbf{v} \cdot \rho_b \ddot{\mathbf{u}}_b d\Omega + \int_{\Sigma} \delta\mathbf{v} \cdot \mathbf{t}_s(\mathbf{u}_{\text{sc}}(\mathbf{u}_b)) d\Sigma = \int_{\Gamma_{b\sigma}} \delta\mathbf{v} \cdot \bar{\mathbf{t}}_b d\Gamma \tag{10}$$

The virtual work of the internal and the inertial forces of the structure results into the stiffness and the mass matrix of the structure, respectively. As the structure Ω_b occupies a finite domain, the stiffness and the mass matrix as well as the external force vector can be computed using a FE method. The tractions $\mathbf{t}_s(\mathbf{u}_{\text{sc}}(\mathbf{u}_b))$ in the soil on the boundary Σ are computed using a BE method.

Numerical modeling of the bounded domain (the generalized structure)

In a FE formulation, the displacement field $\mathbf{u}_b$ is approximated as $\mathbf{u}_b = \mathbf{N}_b \underline{\mathbf{u}}_b$, where $\mathbf{N}_b$ are the globally defined shape functions and $\underline{\mathbf{u}}_b$ is a vector of the three displacement components at all nodal points. Analogously, the strain vector $\boldsymbol{\varepsilon}$ is approximated as $\boldsymbol{\varepsilon} = \mathbf{L}\mathbf{N}_b \underline{\mathbf{u}}_b$, with $\mathbf{L}$ a matrix which contains derivative operators. The virtual work equation (10) must hold for any virtual displacement field $\delta\mathbf{v}$. Substituting the strain-displacement relations, equation (10) can be elaborated as follows:

$$\mathbf{M}_b \underline{\ddot{\mathbf{u}}}_b(t) + \mathbf{f}_b^{\text{int}}(t) = \mathbf{f}_b^{\text{ext}}(t) - \mathbf{Q}(t) \tag{11}$$

where $\mathbf{M}_b$ is the mass matrix of the structure and $\mathbf{f}_b^{\text{int}}$ denotes the vector of the internal forces. The vector $\mathbf{f}_b^{\text{ext}}$ collects the external forces on $\Gamma_{b\sigma}$ and $\mathbf{Q}(t)$ represents the vector of the soil-structure interaction forces. The displacement vector $\underline{\mathbf{u}}_b$ can be divided into the displacement vector $\underline{\mathbf{u}}_{b1}$ corresponding to the nodes within the structure which are not located on the soil-structure interface Σ and the displacement vector $\underline{\mathbf{u}}_{b2}$ corresponding to the degrees of freedom of the nodes on the interface Σ:

$$\begin{bmatrix} \mathbf{M}_{b_1 b_1} & \mathbf{M}_{b_1 b_2} \\ \mathbf{M}_{b_2 b_1} & \mathbf{M}_{b_2 b_2} \end{bmatrix} \begin{Bmatrix} \underline{\ddot{\mathbf{u}}}_{b_1}(t) \\ \underline{\ddot{\mathbf{u}}}_{b_2}(t) \end{Bmatrix} + \begin{Bmatrix} \mathbf{f}_{b_1}^{\text{int}}(t) \\ \mathbf{f}_{b_2}^{\text{int}}(t) \end{Bmatrix} = \begin{Bmatrix} \mathbf{f}_{b_1}^{\text{ext}}(t) \\ \mathbf{f}_{b_2}^{\text{ext}}(t) \end{Bmatrix} - \begin{Bmatrix} \mathbf{0} \\ \mathbf{Q}_{b_2}(t) \end{Bmatrix} \tag{12}$$

The interaction forces $\mathbf{Q}_{b_2}(t)$ depend on the tractions and displacements on the soil-structure interface Σ and are equal to the convolution integral of the dynamic soil stiffness matrix $\mathbf{S}(t)$ and the displacement vector $\underline{\mathbf{u}}_{b_2}(t)$:

$$\mathbf{Q}_{b_2}(t) = \int_0^t \mathbf{S}(t-\tau)\underline{\mathbf{u}}_{b_2}(\tau)d\tau \tag{13}$$

Numerical modeling of the unbounded linear soil domain

As the unbounded soil domain behaves linearly, the dynamic stiffness coefficients of the soil can be calculated in the frequency domain by means of a boundary element formulation that uses the Green's functions of a horizontally stratified soil. This formulation has been implemented in the computer program MISS (Modélisation d'Interaction Sol-Structure) (Clouteau, 1999).

In a stiffness formulation, the inverse Fourier transform of the dynamic stiffness coefficients from the frequency domain to the time domain must be calculated and the asymptotic value for the frequency approaching infinity must be determined. The difficulties in determining the components of the dynamic stiffness can be avoided using a flexibility formulation. The dynamic flexibility coefficients of the soil in the frequency domain are the inverse of the dynamic soil stiffness coefficients and converge to zero when the frequency approaches infinity.

The displacements of the interface nodes $\underline{\mathbf{u}}_{b_2}(t)$ are equal to the convolution integral of the dynamic flexibility matrix $\mathbf{F}(t)$ and the vector of interaction forces $\mathbf{Q}_{b_2}(t)$:

$$\underline{\mathbf{u}}_{b_2}(t) = \int_0^t \mathbf{F}(t-\tau)\mathbf{Q}_{b_2}(\tau)d\tau \tag{14}$$

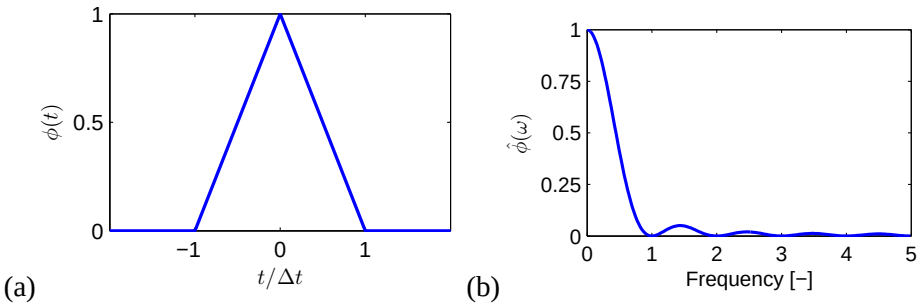

Figure 2: (a) Time history and (b) frequency content of the triangular interpolation function $\phi(t)$.

Introducing a time domain interpolation function $\phi(t)$ (figure 2), the interaction forces $\mathbf{Q}_{b_2}(t)$ are discretized as follows:

$$\mathbf{Q}_{b_2}(t) = \sum_{k=1}^{\infty} \phi(t-k\Delta t)\mathbf{Q}_{b_2}^k \tag{15}$$

Substituting expression (15) into equation (14), the displacement vector $\mathbf{u}_{b_2}^n$ at time $n\Delta t$ becomes:

$$\mathbf{u}_{b_2}^n = \int_0^{n\Delta t} \mathbf{F}(\tau)\left(\sum_{k=1}^{n} \phi((n-k)\Delta t-\tau)\mathbf{Q}_{b_2}^k\right)d\tau \tag{16}$$

This is rearranged as:

$$\mathbf{u}_{b_2}^n = \sum_{k=1}^{n}\left(\int_0^{(n-k+1)\Delta t} \mathbf{F}(\tau)\phi((n-k)\Delta t-\tau)d\tau\right)\mathbf{Q}_{b_2}^k \tag{17}$$

where, due to the bounded support $-\Delta t \leq t \leq \Delta t$ of the time interpolation function $\phi(t)$, the integration bounds are reduced from 0 to $(n-k+1)\Delta t$. The boundary displacement vector $\mathbf{u}_{b_2}^n$ is finally written as:

$$\mathbf{u}_{b_2}^n = \sum_{k=1}^{n} \mathbf{F}^{n-k+1} \mathbf{Q}_{b_2}^k \tag{18}$$

where

$$\mathbf{F}^k = \int_0^{k\Delta t} \mathbf{F}(\tau)\phi((k-1)\Delta t - \tau)d\tau \tag{19}$$

The first dynamic flexibility coefficient $\mathbf{F}^1$ is equal to:

$$\mathbf{F}^1 = \int_0^{\Delta t} \mathbf{F}(\tau)\phi(-\tau)d\tau \tag{20}$$

which results in:

$$\mathbf{F}^1 = \int_{-\infty}^{\infty} \mathbf{F}(\tau)\phi(-\tau)H(\tau)d\tau \tag{21}$$

Introducing the function $\phi'(t) = \phi(t)H(-t)$, where $H(t)$ is the Heaviside step function, the integral is rewritten as:

$$\mathbf{F}^1 = \int_{-\infty}^{\infty} \mathbf{F}(\tau)\phi'(-\tau)d\tau \tag{22}$$

Using the convolution theorem, the flexibility coefficient $\mathbf{F}^1$ is written as:

$$\mathbf{F}^1 = \frac{1}{2\pi} \int_{-\infty}^{\infty} \hat{\mathbf{F}}(\omega)\hat{\phi}'(\omega)d\omega \tag{23}$$

with

$$\hat{\phi}'(\omega) = \frac{1 - e^{i\omega\Delta t} + i\omega\Delta t}{\omega^2 \Delta t} \tag{24}$$

The flexibility coefficient $\mathbf{F}^k$ ($k \geq 2$) in equation (19) can be written as follows:

$$\mathbf{F}^k = \frac{1}{2\pi} \int_{-\infty}^{\infty} \hat{\mathbf{F}}(\omega)\hat{\phi}(\omega)e^{i\omega(k-1)\Delta t}d\omega \tag{25}$$

with

$$\hat{\phi}(\omega) = \frac{2 - 2\cos(\omega\Delta t)}{\omega^2 \Delta t} \tag{26}$$

The integral in equation (23) is evaluated by means of a trapezoidal rule, while equation (25) is evaluated by means of a Filon integration algorithm with an oscillatory kernel function.

The interaction force $\mathbf{Q}_{b_2}^n$ can be elaborated as:

$$\mathbf{Q}_{b_2}^n = (\mathbf{F}^1)^{-1}\mathbf{u}_{b_2}^n - \mathbf{Q}_{b_2}^{\overline{n-1}} \tag{27}$$

where the second term on the right hand side is the time history of the interaction forces:

$$\mathbf{Q}_{b_2}^{\overline{n-1}} = (\mathbf{F}^1)^{-1} \sum_{k=1}^{n-1} \mathbf{F}^{n-k+1} \mathbf{Q}_{b_2}^k \tag{28}$$

Substituting equation (27) into the equation of motion (12) results in:

$$\begin{bmatrix} \mathbf{M}_{b_1b_1} & \mathbf{M}_{b_1b_2} \\ \mathbf{M}_{b_2b_1} & \mathbf{M}_{b_2b_2} \end{bmatrix} \begin{Bmatrix} \ddot{\mathbf{u}}_{b_1}^n \\ \ddot{\mathbf{u}}_{b_2}^n \end{Bmatrix} + \begin{Bmatrix} \mathbf{f}_{b_1}^{\text{int}n} \\ \mathbf{f}_{b_2}^{\text{int}n} \end{Bmatrix} + \begin{bmatrix} \mathbf{0} & \mathbf{0} \\ \mathbf{0} & (\mathbf{F}^1)^{-1} \end{bmatrix} \begin{Bmatrix} \mathbf{u}_{b_1}^n \\ \mathbf{u}_{b_2}^n \end{Bmatrix} = \begin{Bmatrix} \mathbf{f}_{b_1}^{\text{ext}n} \\ \mathbf{f}_{b_2}^{\text{ext}n} \end{Bmatrix} + \begin{Bmatrix} \mathbf{0} \\ \mathbf{Q}_{b_2}^{\overline{n-1}} \end{Bmatrix} \tag{29}$$

Interface modes and interaction forces

A modal reduction technique is applied where the vector of the interface displacements $\mathbf{u}_{b_2}$ is decomposed as a linear combination of vibration modes $\boldsymbol{\psi}_{b_2 m}(m = 1, \ldots, q)$:

$$\mathbf{u}_{b_2} \simeq \sum_{m=1}^{q} \boldsymbol{\psi}_{b_2 m} \alpha_{sm} = \boldsymbol{\Psi}_{b_2} \boldsymbol{\alpha}_s \tag{30}$$

where the modes $\boldsymbol{\psi}_{b_2 m}(m = 1, \ldots, q)$ are collected in a matrix $\boldsymbol{\Psi}_{b_2}$ and the modal coordinates $\alpha_{sm}(m = 1, \ldots, q)$ are collected in a vector $\boldsymbol{\alpha}_s$. The modal coordinates $\boldsymbol{\alpha}_s$ are equal to:

$$\boldsymbol{\alpha}_s = \mathbf{T}_u \mathbf{u}_{b_2} \tag{31}$$

where $\mathbf{T}_u = (\boldsymbol{\Psi}_{b_2}^T \boldsymbol{\Psi}_{b_2})^{-1} \boldsymbol{\Psi}_{b_2}^T$. The modal interaction forces $\mathbf{f}_s$ are introduced as:

$$\mathbf{f}_s = \boldsymbol{\Psi}_{b_2}^T \mathbf{Q}_{b_2} \tag{32}$$

Therefore, the interaction forces $\mathbf{Q}_{b_2}$ can be rewritten as follows in terms of the modal interaction forces:

$$\mathbf{Q}_{b_2} = \mathbf{T}_q \mathbf{f}_s \tag{33}$$

where $\mathbf{T}_q = \boldsymbol{\Psi}_{b_2} (\boldsymbol{\Psi}_{b_2}^T \boldsymbol{\Psi}_{b_2})^{-1}$.

As the dynamic soil stiffness coefficients are usually computed in the frequency domain in terms of the interface modes, equation (18) can be represented in the following modal form:

$$\boldsymbol{\alpha}_s^n = \sum_{k=1}^{n} \mathbf{F}^{n-k+1} \mathbf{f}_s^k \tag{34}$$

where the modal interaction forces $\mathbf{f}_s^n$ can be written as:

$$\mathbf{f}_s^n = (\mathbf{F}^1)^{-1} \boldsymbol{\alpha}_s^n - (\mathbf{F}^1)^{-1} \sum_{k=1}^{n-1} \mathbf{F}^{n-k} \mathbf{f}_s^k \tag{35}$$

where $(\mathbf{F}^1)^{-1}$ denotes the instantaneous dynamic impedance of the unbounded soil domain Ω_s^{ext}. Substituting equation (35) into equation (33) results in:

$$\mathbf{Q}_{b_2}^n = \mathbf{T}_q (\mathbf{F}^1)^{-1} \mathbf{T}_u \mathbf{u}_{b_2}^n - \mathbf{Q}_{b_2}^{\overline{n-1}} \tag{36}$$

where

$$\mathbf{Q}_{b_2}^{\overline{n-1}} = \mathbf{T}_q (\mathbf{F}^1)^{-1} \sum_{k=1}^{n-1} \mathbf{F}^{n-k} \mathbf{f}_s^k \tag{37}$$

Substituting equation (37) into the equation of motion (12) results in:

$$\begin{bmatrix} \mathbf{M}_{b_1 b_1} & \mathbf{M}_{b_1 b_2} \\ \mathbf{M}_{b_2 b_1} & \mathbf{M}_{b_2 b_2} \end{bmatrix} \begin{Bmatrix} \ddot{\mathbf{u}}_{b_1}^n \\ \ddot{\mathbf{u}}_{b_2}^n \end{Bmatrix} + \begin{Bmatrix} \mathbf{f}_{b_1}^{\text{int}\,n} \\ \mathbf{f}_{b_2}^{\text{int}\,n} \end{Bmatrix} + \begin{bmatrix} \mathbf{0} & \mathbf{0} \\ \mathbf{0} & \mathbf{T}_q (\mathbf{F}^1)^{-1} \mathbf{T}_u \end{bmatrix} \begin{Bmatrix} \mathbf{u}_{b_1}^n \\ \mathbf{u}_{b_2}^n \end{Bmatrix} = \begin{Bmatrix} \mathbf{f}_{b_1}^{\text{ext}\,n} \\ \mathbf{f}_{b_2}^{\text{ext}\,n} \end{Bmatrix} + \begin{Bmatrix} \mathbf{0} \\ \mathbf{Q}_{b_2}^{\overline{n-1}} \end{Bmatrix} \tag{38}$$

Modal decomposition

Assuming a linear elastic behaviour for the structure and introducing a modal decomposition based on the modes of the structure with free boundary conditions:

$$\begin{Bmatrix} \mathbf{u}_{b_1} \\ \mathbf{u}_{b_2} \end{Bmatrix} = \begin{Bmatrix} \boldsymbol{\Psi}_{b_1} \\ \boldsymbol{\Psi}_{b_2} \end{Bmatrix} \boldsymbol{\alpha}_s \tag{39}$$

the equation of motion (38) can be elaborated as:

$$\mathbf{I}_{qq}\ddot{\boldsymbol{\alpha}}_s^n + \left(\boldsymbol{\Lambda}_{qq} + (\mathbf{F}^1)^{-1}\right)\boldsymbol{\alpha}_s^n = \boldsymbol{\Psi}_{b_1}^{\mathrm{T}}\mathbf{f}_{b_1}^{\mathrm{ext}n} + \boldsymbol{\Psi}_{b_2}^{\mathrm{T}}\mathbf{f}_{b_2}^{\mathrm{ext}n} + \mathbf{f}_s^{\overline{n-1}} \tag{40}$$

where the q-dimensional diagonal matrix $\boldsymbol{\Lambda}_{qq} = \mathrm{diag}(\omega_m^2)$ contains the squares of the eigenfrequencies $\omega_m (m = 1,\ldots,q)$ and the q-diagonal unit matrix $\mathbf{I}_{qq}$ reflects the orthogonality of the eigenmodes with respect to the mass matrix. The vector $\mathbf{f}_s^{\overline{n-1}}$ is defined as:

$$\mathbf{f}_s^{\overline{n-1}} = (\mathbf{F}^1)^{-1}\sum_{k=1}^{n-1}\mathbf{F}^{n-k}\mathbf{f}_s^k \tag{41}$$

Craig-Bampton substructuring technique

The Craig-Bampton substructuring technique is a valuable alternative to solve the coupled linear problem (Craig & Bampton, 1968). The displacement vector of the structure can be written as:

$$\left\{ \begin{array}{c} \mathbf{u}_{b_1} \\ \mathbf{u}_{b_2} \end{array} \right\} = \left[\begin{array}{cc} \boldsymbol{\Psi}_{b_1} & \boldsymbol{\Psi}_{b_1}^s \\ 0 & \boldsymbol{\Psi}_{b_2} \end{array} \right] \left\{ \begin{array}{c} \boldsymbol{\alpha}_{b_1} \\ \boldsymbol{\alpha}_{b_2} \end{array} \right\} \tag{42}$$

The displacement vector $\mathbf{u}_{b_2}$ is written as a superposition of the modes $\boldsymbol{\Psi}_{b_2}$ of the soil-structure interface. The displacement vector $\mathbf{u}_{b_1}$ is decomposed as a linear combination of the eigenmodes $\boldsymbol{\Psi}_{b_1}$ of the structure fixed on the soil-structure interface and the quasi-static transmission $\boldsymbol{\Psi}_{b_1}^s$ of the modes $\boldsymbol{\Psi}_{b_2}$ of the soil-structure interface:

$$\boldsymbol{\Psi}_{b_1}^s = -\mathbf{K}_{b_1b_1}^{-1}\mathbf{K}_{b_1b_2}\boldsymbol{\Psi}_{b_2} \tag{43}$$

Applying the Craig-Bampton decomposition technique, the equation of motion (38) is represented as:

$$\begin{aligned} &\left[\begin{array}{cc} \mathbf{I}_{kk} & \boldsymbol{\Psi}_{b_1}^T \left[\begin{array}{cc} \mathbf{M}_{b_1b_1} & \mathbf{M}_{b_1b_2} \end{array} \right] \left[\begin{array}{c} \boldsymbol{\Psi}_{b_1}^s \\ \boldsymbol{\Psi}_{b_2} \end{array} \right] \\ \left[\begin{array}{cc} \boldsymbol{\Psi}_{b_1}^{sT} & \boldsymbol{\Psi}_{b_2}^T \end{array} \right] \left[\begin{array}{c} \mathbf{M}_{b_1b_1} \\ \mathbf{M}_{b_2b_1} \end{array} \right] \boldsymbol{\Psi}_{b_1} & \boldsymbol{\Psi}_{b_2}^T\mathbf{M}_{b_2b_2}^s\boldsymbol{\Psi}_{b_2} \end{array} \right] \left\{ \begin{array}{c} \ddot{\boldsymbol{\alpha}}_{b_1}^n \\ \ddot{\boldsymbol{\alpha}}_{b_2}^n \end{array} \right\} + \\ &\left[\begin{array}{cc} \boldsymbol{\Lambda}_{kk} & \mathbf{0} \\ \mathbf{0} & \boldsymbol{\Psi}_{b_2}^T\mathbf{K}_{b_2b_2}^s\boldsymbol{\Psi}_{b_2} + (\mathbf{F}^1)^{-1} \end{array} \right] \left\{ \begin{array}{c} \boldsymbol{\alpha}_{b_1}^n \\ \boldsymbol{\alpha}_{b_2}^n \end{array} \right\} = \left\{ \begin{array}{c} \boldsymbol{\Psi}_{b_1}^T\mathbf{f}_{b_1}^{\mathrm{ext}n} \\ \boldsymbol{\Psi}_{b_1}^{sT}\mathbf{f}_{b_1}^{\mathrm{ext}n} + \boldsymbol{\Psi}_{b_2}^T\mathbf{f}_{b_2}^{\mathrm{ext}n} \end{array} \right\} + \left\{ \begin{array}{c} \mathbf{0} \\ \mathbf{f}_s^{\overline{n-1}} \end{array} \right\} \end{aligned} \tag{44}$$

where the k-dimensional diagonal matrix $\boldsymbol{\Lambda}_{kk} = \mathrm{diag}(\omega_j^2)$ contains the squares of the eigenfrequencies ω_j^2. The matrix $\mathbf{I}_{kk}$ is a k-dimensional unit matrix reflecting the orthogonality of the eigenmodes with respect to the mass matrix. The matrices $\mathbf{M}_{b_2b_2}^s$ and $\mathbf{K}_{b_2b_2}^s$ are the Schur complement of the mass and the stiffness matrices of the structure, respectively.

NUMERICAL EXAMPLES

In order to validate the present method, different linear analyses are performed due to a harmonic loading. Results computed by the present method are compared with those obtained by solution in the frequency domain.

A single pile embedded in a homogeneous half space

A circular concrete pile with a diameter $d_p = 0.50\,\mathrm{m}$ is considered (figure 3a). The pile has a length $L_p = 10\,\mathrm{m}$, a Young's modulus $E_p = 40000\,\mathrm{MPa}$, a Poisson's ratio $\nu_p = 0.25$, and a density $\rho_p = 2500\,\mathrm{kg/m^3}$. The pile is assumed to be completely embedded in the soil with a penetration depth $e_p = 10\,\mathrm{m}$. The longitudinal wave velocity in the pile is equal to $C_p = 4000\,\mathrm{m/s}$.

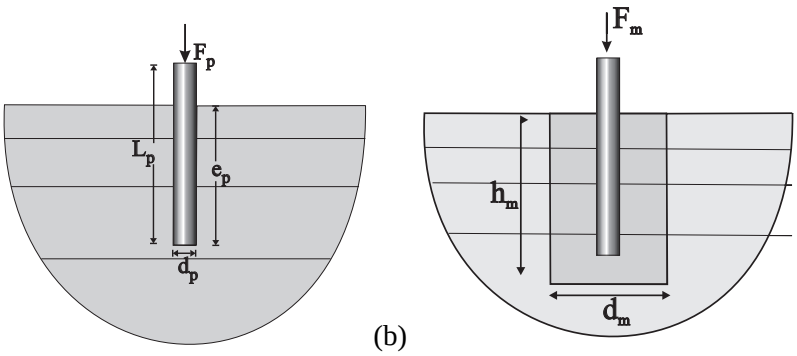

Figure 3: (a) The geometry of a single pile and (b) the geometry of the generalised structure (a single pile and the soil) embedded in a homogeneous half space.

The pile is modeled using 8-node isoparametric brick elements. As the pile has a cylindrical shape and an axial force is applied at the center of the pile, only the axisymmetric modes consisting of the vertical rigid body mode and the flexible axial modes of the pile are considered. Figure 4 shows the flexible axial eigenmodes of the pile with free boundary conditions.

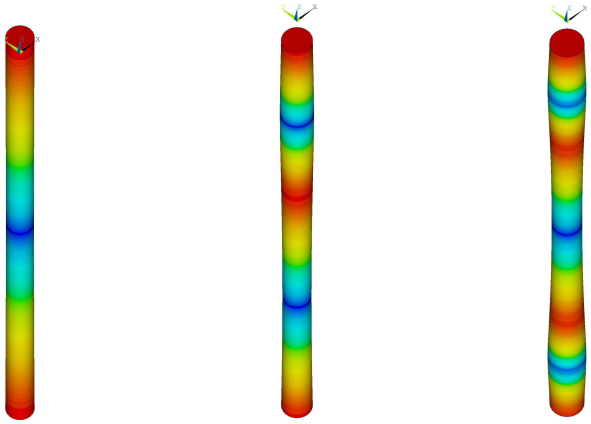

Mode 2: 200.0 Hz Mode 3: 400.3 Hz Mode 4: 601.1 Hz

Figure 4: First three flexible axial modes of the pile with free boundary conditions.

The soil medium consists of a homogeneous half space with a Young's modulus $E_s = 80\,\text{MPa}$, a Poisson's ratio $\nu_s = 0.4$, a material damping ratio $\beta_s = 0.05$, and a density $\rho_s = 2000\,\text{kg/m}^2$. The shear wave velocity in the elastic soil is equal to 120 m/s.

The dynamic soil stiffness matrix is calculated in the frequency domain using a BE method implemented in the program MISS 6.3. The boundary element analysis is applied to compute the impedance functions of the soil. The size of the boundary elements on the soil-pile interface is limited to 0.05 m at the pile toe and 0.25 m along the pile shaft. The impedance functions are computed up to a maximum frequency $f_{\text{max}} = 300\,\text{Hz}$. Figure 5 shows the diagonal elements of the dynamic flexibility matrix. The dynamic flexibility coefficients tend to zero for limiting high frequencies.

The discrete flexibility coefficient matrices in the time domain are computed by the convolution equation (25) with a time step of $\Delta t = 1.7 \times 10^{-3}\,\text{s}$ (figure 6). The number of time steps is selected considering the time that the shear wave needs to pass through the largest dimension of the soil-structure interface. The flexibility coefficients are evaluated by the integration of the product of the dynamic flexibility

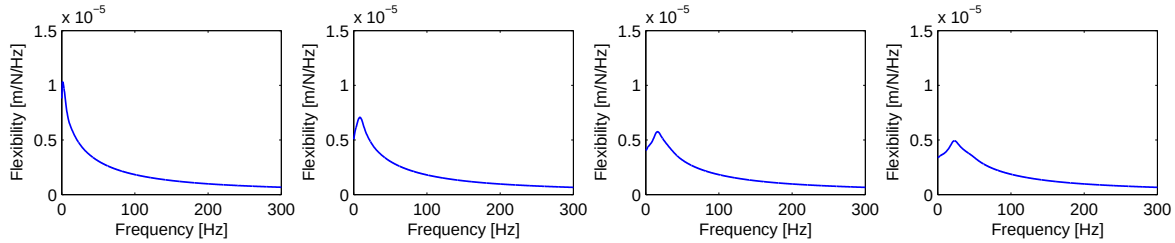

Figure 5: Diagonal elements of the dynamic flexibility matrix in the frequency domain.

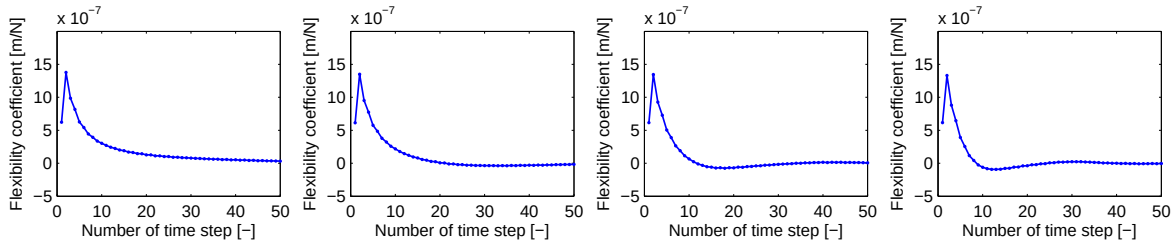

Figure 6: Diagonal elements of the flexibility coefficient matrix in the time domain.

matrix with the frequency content of the triangular or modified triangular shape function. As the upper frequency limit is 300 Hz instead of infinity, an error is induced which has no significant influence on the results when the upper frequency limit is higher than the maximum frequency content of the loading.

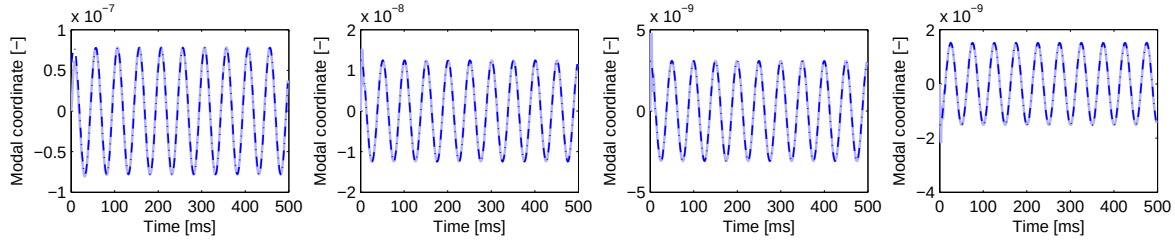

Figure 7: Modal response of the pile subjected to a sinusoidal force with a frequency of 20 Hz, computed by the hybrid method (solid line) and by solution in the frequency domain (dash line).

A vertical sinusoidal force $p(t) = \sin(2\pi ft)$ is considered with a frequency $f = 20\,\text{Hz}$. The force is applied at the pile head. The dynamic response of the pile is computed using a modal reduction technique (equation (40)). Newmark's method is used to solve the equation of motion with a time step $\Delta t = 1.7 \times 10^{-3}\,\text{s}$ and parameters $\alpha = 0.47$ and $\delta = 0.70$. Since the displacements in each time step implicitly depends on the displacements at all previous time steps, unconditional stability can not be guaranteed with a constant average acceleration scheme ($\alpha = 1/4$ and $\delta = 1/2$). For a fixed $\delta > 1/2$, one can select α such that high-frequency dissipation is maximized (Hughes, 1987). It is observed that the better stability is achieved by selecting $\alpha > 0.32(\delta + 1/2)^2$.

Figure 7 shows that the modal response of the pile, computed with the present method, compares well with results obtained in the frequency domain. This good agreement is also preserved when the vertical displacement of the pile head is computed by means of modal superposition (figure 8).

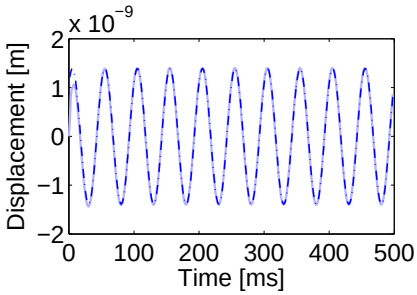

Figure 8: Response of the pile head subjected to a sinusoidal force with a frequency of 20 Hz, computed by the hybrid method (solid line) and by solution in the frequency domain (dash line).

A generalized structure (single pile and soil) embedded in a homogeneous half space

In the following, the pile foundation and a part of the soil are modeled as a generalised structure embedded in a homogeneous half space. The soil-structure system is decomposed into two subdomains: a bounded domain contains the pile and a part of the soil around the pile and an unbounded soil domain. The properties of the pile and the soil are the same as in the previous example (figure 3b). The pile-soil model has a diameter $d_m = 2.00\,\mathrm{m}$ and a height $h_m = 11.0\,\mathrm{m}$. Since the model has a cylindrical geometry and a vertical force is applied at the center of the pile head, the pile and the soil are modeled using 4-node plane axisymmetric finite elements.

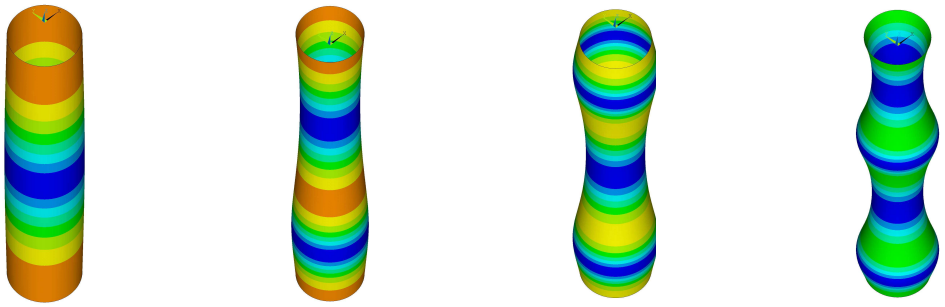

Mode 2. Mode 3. Mode 4. Mode 5.

Figure 9: Some axisymmetric modes of the interface.

The boundary element method is applied to compute the impedance of the unbounded domain. A three-dimensional BE mesh of the interface is built corresponding to the nodes on the interface in the two-dimensional axisymmetric FE mesh. The size of the boundary elements is limited to $0.10\,\mathrm{m}$ at the base and $0.25\,\mathrm{m}$ along the shaft. A rigid body mode in the $z-$direction and 29 flexible modes are selected. The flexible modes in figure 9 illustrate the eigenmodes of the interface with free boundary conditions.

The dynamic response of the generalised structure due to a sinusoidal force is investigated using the Craig-Bampton technique (equation (44)). Results are computed applying 30 interface modes and 200 modes of the structure clamped on the soil-structure interface. Newmark's method is used to solve the equation of motion with a time step $\Delta t = 1.7 \times 10^{-3}\,\mathrm{s}$ and parameters $\alpha = 0.47$ and $\delta = 0.70$. Figure 10 shows the vertical displacement of the pile head due to a sinusoidal excitation. The pile response shows a good agreement with the result of the previous example.

Ground vibrations due to vibratory driving are considered. A standard hydraulic vibratory driver ICE 44-

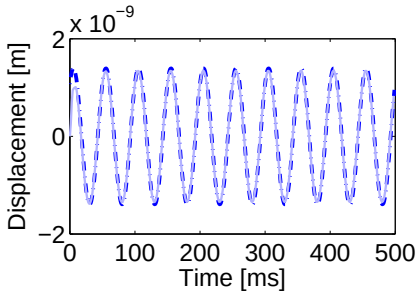

Figure 10: Response of the pile head subjected to a sinusoidal force at 20 Hz, computed by the hybrid method in a pile-soil model (solid line) and by solution in a single pile model (dash line).

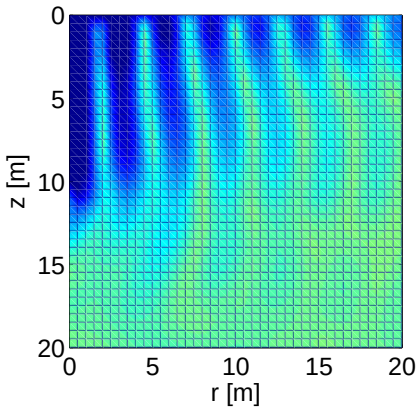

Figure 11: The norm of the particle velocity in a homogeneous half space due to vibratory driving.

30V is selected. It operates at a frequency $f = 20\,\text{Hz}$ with an eccentric moment $me = 50.7\,\text{kgm}$, resulting in a centrifugal force $F_p = 800\,\text{kN}$. In this example, the same Newmark parameters and time step as in the previous example are considered.

Figure 11 shows the norm of the particle velocity in a homogeneous half space due to vibratory pile driving at 20 Hz for the penetration depth $e_p = 10\,\text{m}$. Results are presented in the (r,z) plane, where the vertical coordinate varies from $z = 0.0\,\text{m}$ on the ground surface to $z = 20\,\text{m}$; the horizontal coordinate varies from the soil-structure interface at $r = 1.0\,\text{m}$ up to a distance $r = 20.0\,\text{m}$ from the pile centre. It is observed that: (1) because of the soil-shaft contact, vertically polarized shear waves are generated which propagate radially from the shaft on a cylindrical surface; (2) at the pile toe, shear and compression waves propagate in all directions from the toe on a spherical wave front; and (3) Rayleigh waves propagate radially on a cylindrical wave front along the surface.

Figure 12a illustrates the decrease of the peak particle velocity (PPV) at the surface with the distance r from the pile for the penetration depth $e_p = 10\,\text{m}$. Figure 12b displays the variation of the PPV versus the depth at a distance of $r = 5\,\text{m}$. Results of the hybrid method are compared with those obtained by means of the direct inverse Fourier transformation (Masoumi, et al., 2007). The response along the surface shows a small discrepancy with the reference solution.

CONCLUSION

A hybrid frequency-time domain approach has been proposed to solve a dynamic soil-pile interaction problem in the time domain. Different analyses were performed to investigate the dynamic response of

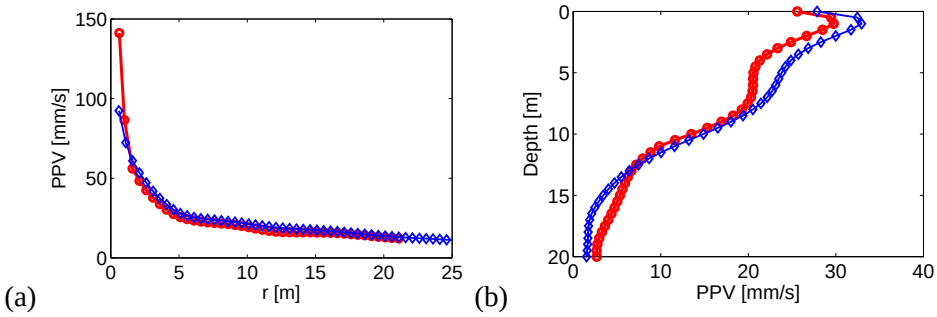

Figure 12: (a) PPV versus the distance from the pile at the free surface, and (b) PPV versus the depth at $r = 5$ m from the pile due to vibratory pile driving at 20 Hz. Results of the hybrid method ($-\circ-$) are compared with those obtained by a frequency domain solution ($-\diamond-$).

a pile under harmonic loading. Results of the present method under linear behaviour were compared with those obtained by a frequency domain analysis and show a good agreement. The prediction of free field vibrations due to vibratory pile driving is illustrated in an example. In the near future, the proposed model will also be applied for a non-linear analysis of an impact pile driving problem.

REFERENCES

C. Bode, et al. (2002). 'Soil-structure interaction in the time domain using halfspace Green's functions'. *Soil Dynamics and Earthquake Engineering* **22**:283–295.

D. Clouteau (1999). *MISS Revision 6.2, Manuel Scientifique*. Laboratoire de Mécanique des Sols, Structures et Matériaux, Ecole Centrale de Paris.

R. Craig & M. Bampton (1968). 'Coupling of substructures for dynamic analyses'. *AIAA Journal* **6**(7):1313–1319.

S. François & G. Degrande (2005). 'Non-linear dynamic soil-structure interaction in the time domain: response of a structure with a disk foundation'. Tech. Rep. BWM-2005-03, Department of Civil Engineering, K.U.Leuven. Research assistantship FWO Flanders.

A. Holeyman (2002). 'Soil behavior under vibratory driving'. In *Proceedings of the International Conference on Vibratory Pile Driving and Deep Soil Compaction, Transvib 2002*, pp. 3–19, Louvain-la-Neuve, Belgium. Keynote lecture.

T. Hughes (1987). *The finite element method, Linear static and Dynamic finite element analysis*. Prentice-Hall, Englewood Cliffs, New Jersey.

S. Mamoon & P. Banerjee (1992). 'Time-domain analysis of dynamically loaded single piles'. *Journal of Engineering Mechanics, Proceedings of the ASCE* **118**(1):140–160.

H. Masoumi, et al. (2007). 'Prediction of free field vibrations due to pile driving using a dynamic soil-structure interaction formulation'. *Soil Dynamics and Earthquake Engineering* **27**:126–143.

L. Tham, et al. (1996). 'Analysis of the transient response of vertically loaded single piles by time domain BEM'. *Computers and Geotechnics* **19**(2):117–136.

J. Wolf (1988). *Soil-structure-interaction analysis in the time domain*. Prentice-Hall, Englewood Cliffs, New Jersey.